Am J Physiol Endocrinol Metab 319: E427–E437, 2020.
First published July 14, 2020; doi:10.1152/ajpendo.00094.2020.

RESEARCH ARTICLE

Ovariectomy modifies lipid metabolism of retroperitoneal white fat in rats: a proteomic approach

Valter T. Boldarine,[1] Amanda P. Pedroso,[1] Caroline Brandão-Teles,[2] Edson G. LoTurco,[6] Cláudia M. O. Nascimento,[1] Lila M. Oyama,[1] Allain A. Bueno,[7] Daniel Martins-de-Souza,[2,3,4,5] and Eliane B. Ribeiro[1]

[1]*Departamento de Fisiologia, Escola Paulista de Medicina, Universidade Federal de São Paulo, São Paulo, Brazil;* [2]*Laboratory of Neuroproteomics, Department of Biochemistry and Tissue Biology, Institute of Biology, University of Campinas (UNICAMP), Campinas, Brazil;* [3]*Instituto Nacional de Biomarcadores em Neuropsiquiatria (INBION) Conselho Nacional de Desenvolvimento Científico e Tecnológico, São Paulo, Brazil;* [4]*Experimental Medicine Research Cluster (EMRC), University of Campinas, Campinas, Brazil;* [5]*D'Or Institute for Research and Education (IDOR), São Paulo, Brazil;* [6]*Divisão de Urologia e Reprodução Humana, Departamento de Cirurgia, Escola Paulista de Medicina, Universidade Federal de São Paulo, São Paulo, Brazil; and* [7]*Department of Biological Sciences, College of Health, Life and Environmental Sciences, University of Worcester, Worcester, United Kingdom*

Submitted 11 March 2020; accepted in final form 14 July 2020

Boldarine VT, Pedroso AP, Brandão-Teles C, LoTurco EG, Nascimento CM, Oyama LM, Bueno AA, Martins-de-Souza D, Ribeiro EB. Ovariectomy modifies lipid metabolism of retroperitoneal white fat in rats: a proteomic approach. *Am J Physiol Endocrinol Metab* 319: E427–E437, 2020. First published July 14, 2020; doi: 10.1152/ajpendo.00094.2020.—Menopause is often accompanied by visceral obesity. With the aim of exploring the consequences of ovarian failure on visceral fat, we evaluated the effects of ovariectomy and estrogen replacement on the proteome/phosphoproteome and on the fatty acid profile of the retroperitoneal adipose depot (RAT) of rats. Eighteen 3-mo-old female Wistar rats were either ovariectomized or sham operated and fed with standard chow for 3 mo. A subgroup of ovariectomized rats received estradiol replacement. RAT samples were analyzed with data-independent acquisitions LC-MS/MS, and pathway analysis was performed with the differentially expressed/phosphorylated proteins. RAT lipid profile was analyzed by gas chromatography. Ovariectomy induced high adiposity and insulin resistance and promoted alterations in protein expression and phosphorylation. Pathway analysis showed that five pathways were significantly affected by ovariectomy, namely, metabolism of lipids (including fatty acid metabolism and mitochondrial fatty acid β-oxidation), fatty acyl-CoA biosynthesis, innate immune system (including neutrophil degranulation), metabolism of vitamins and cofactors, and integration of energy metabolism (including ChREBP activates metabolic gene expression). Lipid profile analysis showed increased palmitic and palmitoleic acid content. The analysis of the data indicated that ovariectomy favored lipogenesis whereas it impaired fatty acid oxidation and induced a proinflammatory state in the visceral adipose tissue. These effects are consistent with the findings of high adiposity, hyperleptinemia, and impaired insulin sensitivity. The observed alterations were partially attenuated by estradiol replacement. The data point to a role of disrupted lipid metabolism in adipose tissue in the genesis of obesity after menopause.

estrogen replacement; lipid profile; menopause; proteome/phosphoproteome; retroperitoneal adipose tissue

INTRODUCTION

The cessation of ovarian hormone production in menopause is often followed by increased body weight gain and adiposity, associated with obesity-related comorbidities (11, 28). In both humans and rodents, a role of estrogens in metabolic, immune, and inflammatory processes has been established, although the complexity by which these effects occur is not fully understood (20, 45). The lack of estrogens after menopause has been associated with a shift of fat distribution from subcutaneous to visceral, with impairment of the sensitivity to insulin and leptin and predisposition to diabetes and to anxiety and depressive disorders (5, 14, 23).

In both humans and rats, the visceral (or abdominal) adipose tissue comprises mesenteric, retroperitoneal, perirenal, and gonadal depots. Additionally, humans have the omental depot (38). A depot specificity of functions has been described for the adipose tissue, which may result from differences intrinsic to preadipocytes and to factors secreted by neighboring organs (62). During the development of obesity, the visceral adipose tissue suffers a higher degree of hypertrophy and macrophage infiltration than the subcutaneous depots, leading to a high production of inflammatory mediators that contribute substantially to the pathophysiology of obesity complications (40, 46).

Several disruptions of the metabolism of visceral adipose tissue have been reported in ovariectomized rodent models. Increased conversion of cortisone to cortisol, due to increased expression of type 1 11β-hydroxysteroid dehydrogenase, has been found in visceral but not subcutaneous adipose depots, contributing to fat redistribution (3). Decreased glutathione peroxidase activity and superoxide dismutase protein levels, indicating impairment of antioxidant status, as well as low mRNA levels of the anti-inflammatory hormone adiponectin, have also been observed (1).

Using a two-dimensional gel electrophoresis-based proteomic approach, a recent study described that ovariectomy affected proteins involved in intermediate metabolism, energy transduction, cell structure, and immune system in the perivarian adipose tissue of rats (2). The use of a more sensitive

Correspondence: V. T. Boldarine (valtertadeuboldarine@gmail.com).

and accurate proteomic technique could help unravel a more expressive number of proteins and pathways affected by ovarian failure in the visceral fat. Moreover, the identification of changes in protein phosphorylation is of high relevance, as it plays a pivotal role in a multitude of cellular functions.

Additionally, perturbations of visceral adipose tissue functions have been associated with its fatty acid composition in several conditions, such as diet-induced obesity and diabetes (6, 63). However, data on the effects of obesity induced by the loss of ovarian hormones in visceral adipose tissue fatty acid composition are scarce. One study reported increased levels of short-chain saturated fatty acids in the visceral fat of postmenopausal women (67). Further studies on the subject are necessary.

Aiming at expanding our knowledge of the consequences of ovarian failure on visceral fat, the present study examined the effects of ovariectomy and of estrogen replacement on the proteome/phosphoproteome as well as on the fatty acid profile of the retroperitoneal fat of rats.

MATERIALS AND METHODS

Experimental procedures. The experiments were reviewed and approved by the Committee in Research Ethics of the Universidade Federal de São Paulo (CEUA no.: 2172030315/2016), which follows the guidelines of the Conselho Nacional de Controle de Experimentação Animal (CONCEA). The present data are part of our previously published investigation in which we evaluated the effects of ovariectomy, aligned or not to high-fat diet feeding, on metabolic and behavior parameters of rats (5). Briefly, female Wistar rats (12 wk old) were either ovariectomized (Ovx group, $n = 12$) or sham operated (Sham group, $n = 6$) under ketamine-xylazine anesthesia (66 and 33 mg/kg ip). A subset of Ovx animals (Ovx+E_2 group) received 17β-estradiol replacement via subcutaneous pellets (0.25 mg/pellet, 90-day release; Innovative Research of America, Sarasota, FL). The daily dose of estrogen released was 2.8 μg/day for 90 days, yielding a daily dose range of 0.010 to 0.008 $mg \cdot kg^{-1} \cdot day^{-1}$, considering the mean initial and final body weights during the 12 wk of treatment. One dose of penicillin (60,000 U im) and ibuprofen (1 mg/kg body wt po) was given to all animals after the surgery. Additionally, they received one ibuprofen dose per day for the 2 subsequent days. They were maintained under a 12:12-h light-dark cycle (lights on at 6 AM) and 23 ± 1°C temperature with food (2.87 kcal/g, 15% of energy from fat, Nuvilab CR-1; Nuvital Nutrientes SA, Colombo, Brazil) and water ad libitum for 12 wk. Body weight and 24-h food mass intake were measured once a week. Feed efficiency was calculated as (body weight gain/energy intake) × 100.

Euthanasia was conducted under thiopental anesthesia (80 mg/kg ip) after a 24-h fast. Trunk blood was collected, and white fat pads (retroperitoneal, gonadal, and mesenteric) were dissected, weighed, and frozen in liquid nitrogen. All tissue and serum samples were stored at −80°C. The uteri were weighed for confirmation of completeness of ovary removal.

Serum and tissue cytokine measurements. Serum measurements and Homeostatic Model Assessment (HOMA) index were conducted as previously described (5). Retroperitoneal adipose depot (RAT) contents of TNF-α (sensitivity: 2.4 ng/mL; intra-assay precision: 4.98%; interassay precision: 9.44%) and IL-6 (sensitivity: 0.7 ng/mL; intra-assay precision: 3.96%; interassay precision: 8.64%) were also determined by ELISA (R&D Systems, Minneapolis, MN).

Retroperitoneal fat proteome and phosphoproteome analyses. Aliquots (800 mg) of RAT fat pads were homogenized in 1 mL of buffer containing 50 mM ammonium bicarbonate, 1% sodium deoxycholate (wt/vol), and deionized water (51), with the addition of a protease-phosphatase inhibitor cocktail (Thermo Scientific, Rockford, IL), and centrifuged at 19,000 *g* for 30 min at 4°C. Protein concentration in the supernatants was determined with a Pierce BCA assay (Thermo Scientific, Rockford, IL). Aliquots of 200 μg of protein were diluted in 50 mM ammonium bicarbonate to a final volume of 85 μL. Samples were then subjected to reduction with 2.5 μL of 100 mM DTT at 60°C for 30 min and alkylation with 2.5 μL of 300 mM iodoacetamide at room temperature for 30 min. Proteins were digested overnight with trypsin (Promega, Fitchburg, WI) at a 1:100 (wt/wt) enzyme-to-protein ratio at 37°C. After digestion, samples were centrifuged at 19,000 *g* for 15 min at 4°C, the supernatants were collected, and an equal volume of ethyl acetate was added (36). Then, trifluoroacetic acid was added to a final concentration of 0.5%. Samples were homogenized in vortex and centrifuged at 19,000 *g* for 5 min at 4°C. Supernatants were collected, transferred to Millex-GV filters (Millipore, Burlington, MA), recovered, dried in a vacuum concentrator centrifuge (Eppendorf, Hamburg, Germany), and stored at −80°C until mass spectrometry analysis.

Liquid chromatography-mass spectrometry. After reconstitution of the samples in 1% (vol/vol) formic acid, protein content was determined fluorometrically (Qubit 3.0 Fluorometer; Thermo Scientific, Rockford, IL) and the final concentration was adjusted to 0.5 μg/μL. The proteomic and phosphoproteomic analyses were performed by data-independent acquisitions liquid chromatography-mass spectrometry (ACQUITY UPLC M-Class coupled to Synapt G2-Si mass spectrometer; Waters, Milford, MA). An ACQUITY UPLC HSS T3 nanoACQUITY Column (100 Å, 1.8 μm, 75 μm × 150 mm; Waters) was used for peptide separation (1 μg) in acetonitrile gradient from 7% (vol/vol) for 54 min and then increased to 80% acetonitrile for 13 min, at a flow rate of 500 nL/min. Data were acquired with nanoESI ionization on positive mode, in $HDMS^E$ mode using Transfer MS Collision Energy Low (eV) 19.0 and Transfer MS Collision Energy High (eV) 53.0. Human Glu-fibrinopeptide B was used for mass spectrometer calibration. MS identification was made between 50 and 2,000 mass-to-charge ratio (*m/z*).

Database search. Mass spectrometry data processing and database search against *Rattus norvegicus* sequences (UniProtKB/Swiss-Prot database, https://www.uniprot.org; 8,680 entries) were performed with Progenesis for Proteomics software (version 4.0; Waters). Peptide identification followed the parameters maximum 1 missed cleavage site allowed for trypsin digestion; cysteine carbamidomethylation as fixed modification; and methionine oxidation as variable modification. The search for phosphopeptides was made through variable modification of serine, threonine, and tyrosine phosphorylation. Protein identification used the following criteria: false discovery rate (FDR) set at <1%, minimum of 2 fragment ions per peptide, 5 fragment ions per protein, and 2 peptides per protein. Relative protein quantification was performed by the Hi-N approach, using the three most abundant peptides, with priority of the unique peptides' ones (58). Normalized data were exported to Excel files.

Pathway analysis. The proteins differentially expressed and/or differentially phosphorylated among the groups were included in the test to determine enriched pathways, using the online Panther platform (http://www.pantherdb.org, version 14.1, released 07/11/2019). The whole *R. norvegicus* proteome was used as the reference list, and the Reactome Pathways was used as the annotation data set. Significantly enriched pathways were based on Fisher's exact test followed by Bonferroni correction with significance set to $P < 0.05$.

RAT fatty acid composition. Aliquots of 1,000 mg of RAT were extracted in hexane-isopropanol [3:2 (vol/vol)] containing 0.01% butylated hydroxytoluene (BHT). After addition of chloroform-methanol-water [2:1:1 (vol/vol/vol)], the samples were centrifuged (10,000 *g* for 10 min) and the organic layers were separated and evaporated to complete dryness with oxygen-free nitrogen (OFN). The lipids were partitioned again in chloroform-methanol-water [8:4:3 (vol/vol/vol)], and the chloroform layer was dried under OFN.

Fatty acid analysis was performed as previously described (7). Briefly, fatty acid methyl esters (FAMEs) were obtained by heating

the samples with 15% acyl chloride in dry methanol in a sealed tube at 70°C for 3 h under OFN. A solution of 5% NaCl was used to stop the reaction at room temperature, and FAMEs were extracted by three washings with petroleum ether containing 0.01% BHT. Gas chromatography with flame ionization detector (GC2010 Plus; Shimadzu, Kyoto, Japan) was performed with a TRACE TR-FAME capillary column (Thermo Scientific, Rockford, IL). The intensity of peaks was quantified with the software Labsolutions (Shimadzu, Kyoto, Japan).

Statistical analysis. Body weight, white fat depot mass, and serum parameter variables were tested for normality (Shapiro–Wilk test) and homoscedasticity (Levene's test). Normally distributed variables (means ± SE) were analyzed by ANOVA and Tukey post hoc test. Nonparametric variables (median and interquartile range) were analyzed by Kruskal–Wallis ANOVA followed by two-tailed multiple comparisons. All tests were performed with Statistica 12 Software (StatSoft, Tulsa, OK) for $P < 0.05$.

Proteome and phosphoproteome data were submitted to analysis on the online platform MetaboAnalyst (https://www.metaboanalyst.ca). Data were log transformed, and the missing values were replaced by half the minimum positive value in the original data. The data were normalized by pareto scaling and submitted to principal component analysis (PCA) followed by partial least-squares discriminant analysis (PLSDA). Variable importance for the projection (VIP) values higher than 1.5 in principal component 1 were considered in order to identify the proteins and phosphopeptides that most contributed to discrimination among the groups.

RESULTS

Ovariectomy induced high adiposity and insulin resistance. As shown in Table 1, the success of ovariectomy was confirmed by the low uterus weight of the ovariectomized groups. Initial body weight was similar among the three groups, whereas both ovariectomized groups had higher body weights, feed efficiency, and total fat mass at the end of the 12 wk. Regarding the individual fat depot masses, although the gonadal fat depot was not different among the groups, both retroperitoneal and mesenteric depots were increased by ovariectomy and not normalized by estrogen replacement. The elevations induced by ovariectomy in leptin and insulin levels, leptin-to-adiponectin ratio, HOMA of insulin resistance (HOMA-IR), and HOMA of β-cell function (HOMA-β) were significantly attenuated by estradiol replacement. Total cholesterol, HDL-cholesterol, and triglyceride levels did not differ significantly among the groups. RAT levels of TNF-α and IL-6 were similar among the groups.

Ovariectomy induced changes in protein expression and phosphorylation and modified metabolic pathways in retroperitoneal fat. Among the 18 biological samples, 13,722 peptides, corresponding to 1,246 proteins, were identified, of which 994 proteins met the inclusion criteria and were included in the statistical analysis. The multivariate analysis found 91 RAT proteins significantly modulated among the groups. The PLSDA analysis based on principal components showed a separation between the Sham and Ovx groups, whereas the Ovx+E_2 group presented an intermediate profile (Fig. 1*A*). Forty-two proteins were downregulated and 49 proteins were upregulated by ovariectomy in relation to the Sham group. The E_2-replacement group presented 43 downregulated proteins and 48 upregulated proteins in comparison to the Sham group. The complete list of proteins with altered expression is presented in Supplemental Appendix S1 (all Supplemental Material is available at https://doi.org/10.6084/m9.figshare.12377696.v1).

Considering the phosphoproteome results, 1,074 peptides were identified with at least one phosphorylation site, corresponding to 468 proteins. The multivariate analysis found 107 peptides (corresponding to 96 proteins) with a characteristic phosphorylation pattern for each group. The analysis based on principal components showed a separation of Sham and Ovx groups, whereas the E_2-replacement group was shown to be in an intermediate position (Fig. 1*B*). In comparison to the Sham group, the Ovx group showed decreased phosphorylation of 39 proteins and 68 proteins showed increased phosphorylation. The Ovx+E_2 group

Table 1. *Body and serum parameters*

	Sham	Ovx	Ovx+E_2
Initial body weight, g	264.79 ± 5.22	263.00 ± 3.79	263.51 ± 5.02
Final body weight, g	280.84 (272.38–285.75)	338.00 (336.00–339.50)*	335.71 (325.89–337.00)*
Cumulative food intake, kcal	526.36 ± 14.87	570.90 ± 12.48	613.63 ± 13.01*
Feed efficiency, g/kcal	2.72 ± 0.54	13.52 ± 0.66*	11.98 ± 0.81*
Uterus, g	0.43 ± 0.03	0.11 ± 0.02*	0.15 ± 0.02*
Total fat mass, g	10.37 ± 0.89	17.71 ± 1.22*	15.89 ± 1.11*
Retroperitoneal fat mass, g	3.49 ± 0.30	7.23 ± 0.56*	6.02 ± 0.46*
Mesenteric fat mass, g	1.67 ± 0.17	3.75 ± 1.20*	3.38 ± 0.80*
Periovarian fat mass, g	4.97 ± 0.44	6.15 ± 0.48	5.98 ± 0.49
Leptin, ng/mL	2.17 (1.84–2.61)	10.06 (7.80–012.52)*#	5.97 (4.45–9.89)
Adiponectin, μg/mL	5.65 ± 0.59	8.06 ± 1.04	7.67 ± 0.91
Leptin/adiponectin	0.41 ± 0.06	1.42 ± 0.29*#	0.89 ± 0.18
TNF-α, pg/mg protein	7.04 ± 0.72	7.45 ± 0.78	6.96 ± 2.34
IL-6, pg/mg protein	32.2 ± 5.28	54.6 ± 17.3	26.8 ± 2.62
Glucose, mg/dL	92.80 ± 2.98	105.72 ± 6.38	103.88 ± 6.29
Insulin, ng/mL	0.56 ± 0.06	2.32 ± 0.20*#	1.31 ± 0.12*
HOMA-IR	3.18 (2.32–4.25)	14.37 (12.08–19.07)*#	7.93 (6.26–8.28)
HOMA-β	0.18 (0.14–0.23)	0.52 (0.38–0.72)*#	0.29 (0.24–0.45)
Total cholesterol, mg/dL	115.46 (104.96–121.76)	140.84 (119.08–193.13)	126.34 (119.85–133.97)
HDL cholesterol, mg/dL	205.73 (179.01–251.91)	163.17 (146.18–174.05)	142.37 (135.50–157.63)
Triglycerides, mg/dL	99.18 (94.67–108.20)	111.27 (105.33–118.85)	122.54 (107.79–220.49)

Data are presented as means ± SE for variables with normal distribution or median (interquartile range) (Q1–Q3) for variables not normally distributed; n = 6 animals per group. Ovx, ovariectomized; Ovx+E_2, ovariectomized with 17β-estradiol replacement; HOMA-IR, Homeostatic Model Assessment of insulin resistance; HOMA-β, HOMA of β-cell function; Sham, sham operated. *$P < 0.05$ vs. Sham; #$P < 0.05$ vs. Ovx+E_2.

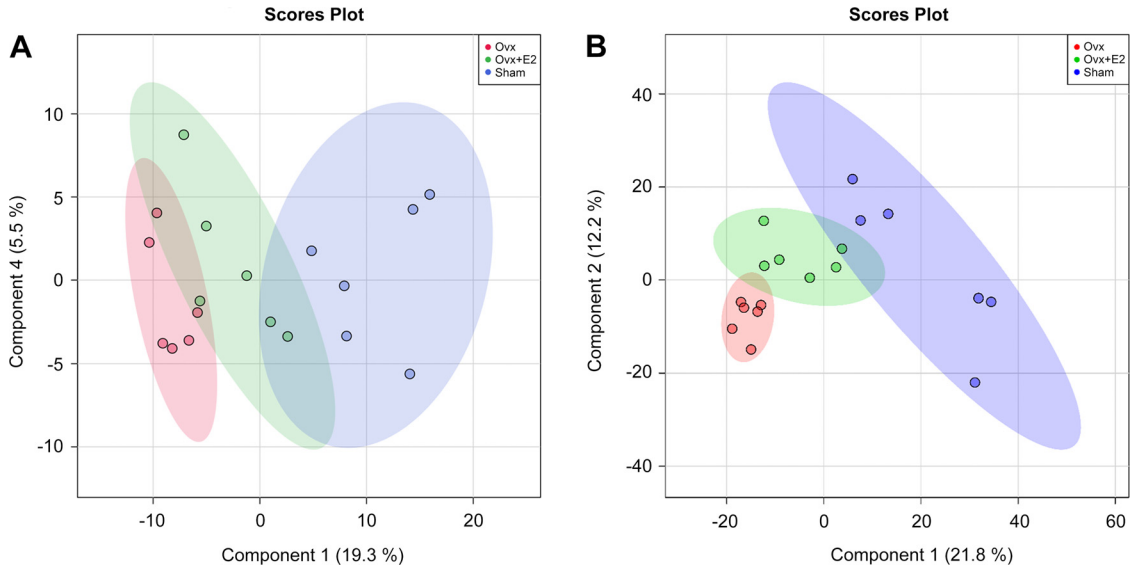

Fig. 1. Separation of the groups with multivariate analyses of proteome data. *A*: supervised partial least-squares discriminant analysis (PLSDA) analyses based on 994 protein intensities. The principal components explaining the separation are *1* and *4*; Q2 = 0.7; R2 = 0.9. *B*: supervised PLSDA analyses based on 1,074 peptide intensities. The principal components explaining the separation are *1* and *2*; Q2 = 0.6; R2 = 0.9. Ovx, ovariectomized; Ovx+E_2, ovariectomized with 17β-estradiol replacement; Sham, sham operated.

showed downregulation of 42 proteins and 65 proteins with increased phosphorylation compared with the Sham group. The complete list of proteins with altered phosphorylation is presented in Supplemental Appendix S2.

The pathway overrepresentation test showed significant enrichment of pathways involved in lipid metabolism: fatty acyl-CoA biosynthesis pathway (1 protein/4 phosphopeptides; P = 2.67E−2) (Fig. 2*A*) and metabolism of lipids pathway (9 proteins/11 phosphopeptides; P = 5.30E−5), the latter including fatty acid metabolism (6 proteins/9 phosphopeptides; P = 7.35E−8) and mitochondrial fatty acid β-oxidation (4 proteins/2 phosphopeptides; P = 1.65E−3) (Fig. 2*B*). The proteins participating in these pathways included long-chain fatty acid-CoA ligase 5 (ACSL5), long-chain-fatty-acid-CoA ligase 1 (ACSL1),

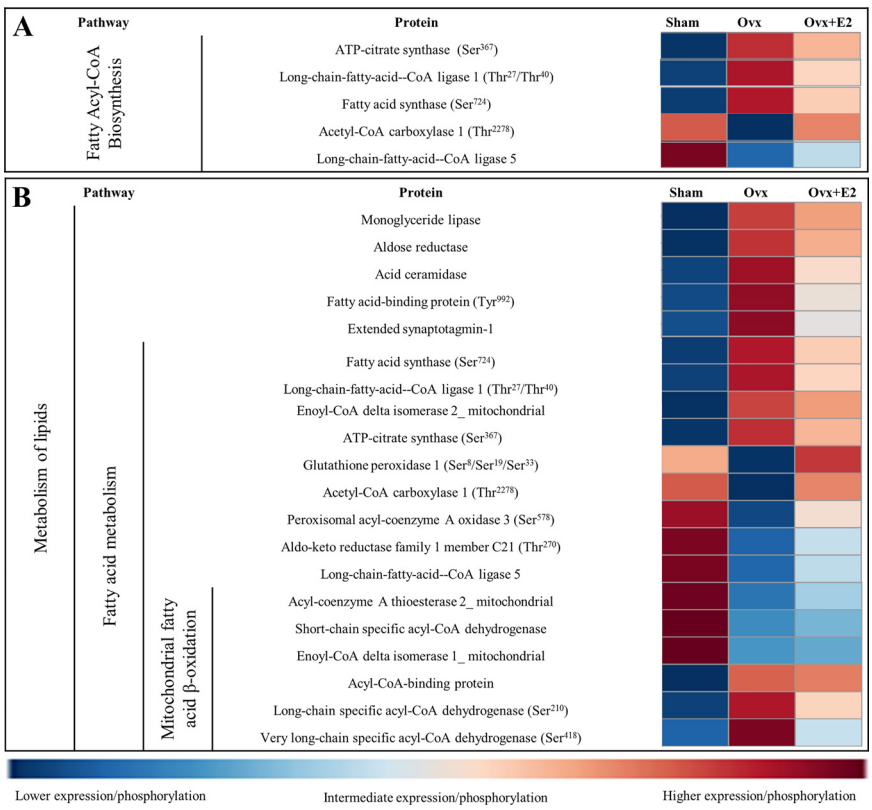

Fig. 2. Representation of the fatty acyl-CoA biosynthesis (*A*) and metabolism of lipids (B) pathways and their associated proteins and phosphopeptides. Pathway enrichment analysis: Fisher's exact test followed by Bonferroni correction. The colored bars indicate the protein expression/phosphorylation peak intensities. All 6 samples in each experimental group were included in the analyses. Ovx, ovariectomized; Ovx+E_2, ovariectomized with 17β-estradiol replacement; Sham, sham operated.

short-chain specific acyl-CoA dehydrogenase (ACADS), long-chain specific acyl-CoA dehydrogenase (ACADL), very long-chain specific acyl-CoA dehydrogenase (ACADVL), acyl-coenzyme A thioesterase type 2 (ACOT2), enoyl-CoA delta isomerase-1 (ECI1), acetyl-CoA carboxylase-1 (ACC1), and fatty acid synthase (FAS) (Table 2).

The innate immune metabolism pathway (10 proteins/16 phosphopeptides; $P = 1.82E-7$), including the neutrophil degranulation pathway (5 proteins/13 phosphopeptides; $P = 2.07E-10$), was also altered by ovariectomy (Fig. 3), and the affected proteins included platelet glycoprotein 4 (CD36). Two other important proteins related to the immune system were adenylyl cyclase-associated protein 1 (CAP1) and class I histocompatibility antigen, non-RT1.A alpha-1 chain (RT1-AW2) (Table 2).

The last two enriched pathways were the metabolism of vitamins and cofactors pathway (5 proteins/4 phosphopeptides; $P = 4.29E-2$) (Fig. 4*A*) and the integration of energy metabolism pathway (3 proteins/6 phosphopeptides; $P = 5.74E-4$), which included the pathway ChREBP activates metabolic gene expression (3 phosphopeptides; $P = 4.42E-2$) (Fig. 4*B*).

Table 2 also shows that ovariectomy induced changes in two proteins related to adipogenesis, all-*trans*-retinol 13,14-reductase (RETSAT) and lipoprotein lipase (LPL), as well as two proteins involved in insulin sensitivity, elongation factor 1-delta (EEF1D) and integrin-β1 (ITB1).

Ovariectomy increased saturated fatty acid content and disturbed the polyunsaturated fatty acid ratios in RAT. The results regarding the fatty acid analyses are depicted in Table 3. The Ovx group showed increased content of lauric, myristic, and palmitic acids in relation to the Sham group. Increased total saturated fatty acids (SFA), alongside increased palmitic-to-stearic ratio, was also found in the Ovx group. Estrogen replacement brought the content of lauric and myristic acids, as well as total SFA, back to levels comparable to the Sham group.

The monounsaturated fatty acid (MUFA) myristoleic and palmitoleic acid levels were higher in the Ovx group compared with the Sham group but comparable to the Sham group when estrogen replacement was introduced. Eicosenoic acid was lower in both Ovx and Ovx+E_2 groups compared with the Sham group. The palmitic-to-palmitoleic ratio was significantly decreased in the Ovx group but normalized in the Ovx+E_2 group.

Ovariectomy led to a significant disturbance in the proportions of various polyunsaturated fatty acids (PUFAs). The essential fatty acids alpha-linolenic and linoleic acids were respectively increased and decreased in the Ovx group compared with the Sham group. Estrogen replacement was successful in returning linoleic acid back to a level comparable to the Sham group, but the same was not found for alpha-linolenic acid. A significant increase in eicosapentaenoic acid (EPA) was found in the Ovx and Ovx+E_2 groups. An increase in arachidonic acid (AA) was also found in both groups compared with the Sham group, but such difference did not reach statistically significant levels.

Ovariectomy increased 0.33% of the total n–3 while decreasing 3% of the total n–6 in comparison to the Sham group. Such differences reached statistically significant levels, and although they remained for total n–3 in the Ovx+E_2 group, they were no longer statistically different for n–6 in the Ovx+E_2 group. The total n–6-to-n–3 ratio was lower in

Table 2. *Highlighted proteins with altered expression and/or phosphorylation*

Protein (phosphosite)	Expression Fold Change			Phosphorylation Fold Change		
	Ovx/Sham	Ovx+E_2/Sham	Ovx+E_2/Ovx	Ovx/Sham	Ovx+E_2/Sham	Ovx+E_2/Ovx
Long-chain fatty acid-CoA ligase 5	0.61	0.72	1.18			
Long-chain fatty acid-CoA ligase 1 (Thr^{27}/Thr^{40})				3.79	2.26	0.60
Short-chain specific acyl-CoA dehydrogenase, mitochondrial	0.59	0.63	1.06			
Long-chain specific acyl-CoA dehydrogenase, mitochondrial (Ser^{210})				27.25	7.84	0.29
Very long-chain specific acyl-CoA dehydrogenase, mitochondrial (Ser^{418})				4.49	1.75	0.39
Acyl-coenzyme A thioesterase 2, mitochondrial	0.62	0.70	1.13			
Enoyl-CoA delta isomerase 1, mitochondrial	0.54	0.56	1.03			
Acetyl-CoA carboxylase (Thr^{2278})				0.12	0.84	7.21
Fatty acid synthase (Ser^{725})				2.82	1.95	0.69
All-*trans*-retinol 13,14-reductase (Ser^{404}/Tyr^{409})	1.75	1.52	0.87	0.96	2.95	3.08
Lipoprotein lipase (Tyr^{191})	2.15	2.03	0.94	1.78	1.04	0.58
Platelet glycoprotein 4	1.53	1.33	0.86			
Adenylyl cyclase-associated protein 1 (Ser^{300}/Thr^{306}/Ser^{307})	2.12	1.01	0.47	18.49	1.20	0.07
Class I histocompatibility antigen, non-RT1.A alpha-1 chain (Ser^{295})	12.80	2.61	0.20	12.79	2.35	0.18
Elongation factor 1-delta (Ser^{447})	0.65	0.76	1.18	0.23	0.34	1.52
Integrin beta-1 (Ser^{263})	0.42	0.57	0.82	2.23	2.27	1.02

Ovx, ovariectomized; Ovx+E_2, ovariectomized with 17β-estradiol replacement; Sham, sham operated.

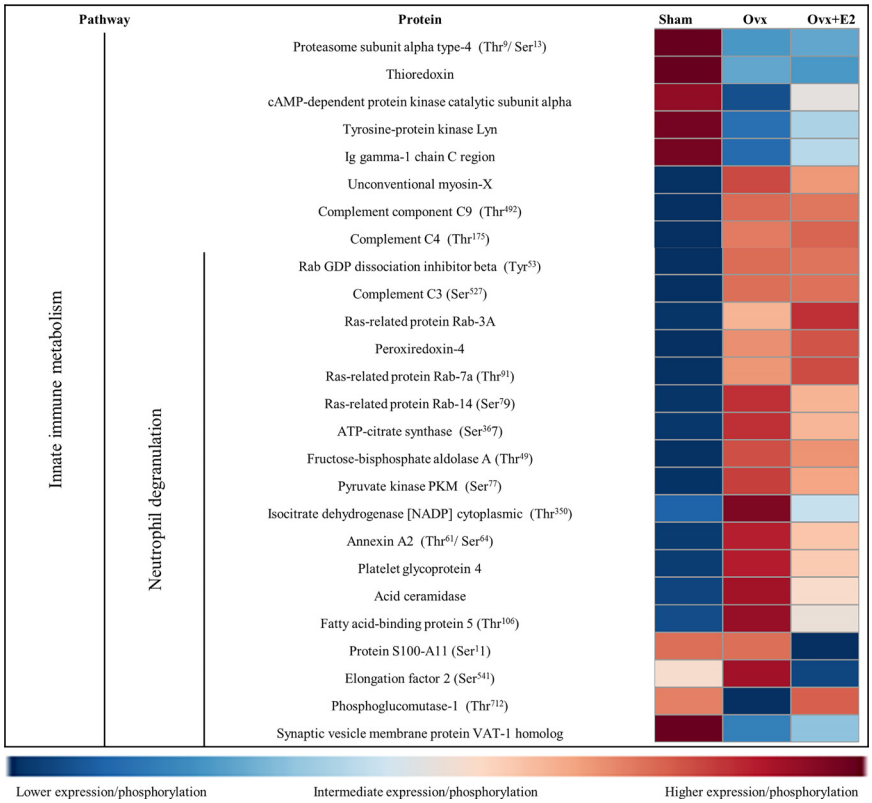

Fig. 3. Representation of the innate immune metabolism pathway and its associated proteins and phosphopeptides. Pathway enrichment analysis: Fisher's exact test followed by Bonferroni correction. The colored bars indicate the protein expression/phosphorylation peak intensities. All 6 samples in each experimental group were included in the analyses. Ovx, ovariectomized; Ovx+E_2, ovariectomized with 17β-estradiol replacement; Sham, sham operated.

Ovx and Ovx+E_2 groups in comparison to the Sham group; however, the total SFA-to-PUFA ratio was higher in Ovx and similar in Ovx+E_2 compared with the Sham group.

DISCUSSION

Menopause has been considered an important factor leading to obesity, mainly due to the shift in fat distribution from subcutaneous to visceral (24). We thus hypothesized that the loss of ovarian hormones could lead to impairment of protein and lipid regulation in the visceral adipose tissue. To test this hypothesis, we used shotgun proteomics, along with fatty acid profiling, to determine proteins and lipids affected and to evaluate the extent to which estrogen replacement would modify the ovariectomy-induced alterations.

In the rat, the visceral adipose tissue is comprised by the retroperitoneal, perirenal, perigonadal, and mesenteric depots (38). Ovariectomy has been shown to induce significant changes in RAT metabolism (1, 12, 49).

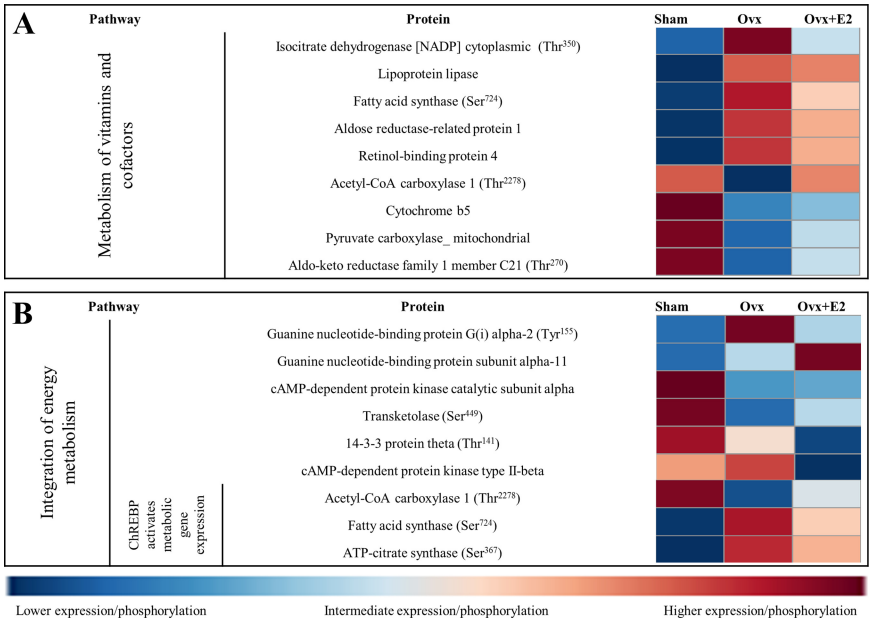

Fig. 4. Representation of the metabolism of vitamins and cofactors (*A*) and integration of energy metabolism (*B*) pathways and their associated proteins and phosphopeptides. Pathway enrichment analysis: Fisher's exact test followed by Bonferroni correction. The colored bars indicate the protein expression/phosphorylation peak intensities. All 6 samples in each experimental group were included in the analyses. Ovx, ovariectomized; Ovx+E_2, ovariectomized with 17β-estradiol replacement; Sham, sham operated.

Table 3. *Fatty acid composition of RAT total lipid*

Fatty Acid		% of Total Fatty Acids		
		Sham	Ovx	Ovx+E_2
C12:0	Lauric acid	0.04 ± 0.01	0.05 ± 0.01*#	0.04 ± 0.01
C14:0	Myristic acid	0.62 ± 0.06	0.75 ± 0.07*#	0.67 ± 0.11
C16:0	Palmitic acid	18.7 ± 1.4	21.2 ± 1.4*	20.4 ± 1.2*
C18:0	Stearic acid	3.35 ± 0.21	3.21 ± 0.37	3.2 ± 0.15
C20:0	Arachidinic acid	0.06 ± 0.01	0.04 ± 0.01*	0.05 ± 0.01*
C22:0	Behenic acid	0.018 ± 0.001	0.009 ± 0.001*#	0.012 ± 0.001*
C16:0/C18:0		5.75 ± 0.39	6.67 ± 0.88*	6.3 ± 0.57
Σ SFA		22.8 ± 1.5	25.3 ± 1.5*#	24.4 ± 1.3
C14:1n–7	Myristoleic acid	0.02 ± 0.01	0.03 ± 0.01*#	0.02 ± 0.01
C16:1n–7	Palmitoleic acid	1.55 ± 0.3	2.36 ± 0.59*#	1.8 ± 0.52
C18:1n–9	Oleic acid	27.7 ± 1.2	27.5 ± 1.7	27.2 ± 0.9
C18:1n7	*cis*-Vaccenic acid	2.32 ± 0.18	2.23 ± 0.12	2.31 ± 0.17
C20:1n9	Eicosenoic acid	0.18 ± 0.02	0.15 ± 0.01*	0.16 ± 0.01*
C18/C18:1		0.11 ± 0.01	0.11 ± 0.02	0.11 ± 0.01
C16:0/C16:1n–7		12.2 ± 1.7	9.38 ± 1.8*#	12.3 ± 2.9
Σ MUFA		31.8 ± 1.3	32.4 ± 2.3	31.4 ± 1.4
C18:3n–3	Alpha-linolenic acid	1.50 ± 0.18	1.81 ± 0.14*	1.84 ± 0.05*
C20:5n–3	Eicosapentaenoic acid (EPA)	0.02 ± 0.01	0.03 ± 0.001*	0.03 ± 0.01*
C22:5n–3	Docosapentaenoic acid (DPA)	0.09 ± 0.02	0.09 ± 0.02	0.09 ± 0.02
C22:6n–3	Docosahexaenoic acid (DHA)	0.16 ± 0.05	0.15 ± 0.06	0.15 ± 0.03
Σ n–3		1.75 ± 0.28	2.08 ± 0.17*	2.11 ± 0.08*
C18:2n–6	Linoleic acid	40.14 ± 2.0	37.1 ± 2.8*	38.5 ± 2.3
C18:3n–6	Gamma-linoleic acid	0.07 ± 0.02	0.1 ± 0.01*	0.09 ± 0.02*
C20:2n–6	Eicosadienoic acid (EDA)	0.19 ± 0.02	0.16 ± 0.03*	0.17 ± 0.2*
C20:3n–6	Dihomo-gamma linoleic acid	0.14 ± 0.02	0.14 ± 0.02	0.15 ± 0.01
C20:4n–6	Arachidonic acid (AA)	0.63 ± 0.17	0.69 ± 0.18	0.74 ± 0.14
C22:4n–6	Docosatetraenoic acid	0.23 ± 0.08	0.19 ± 0.06	0.20 ± 0.04
Σ n–6		41.4 ± 2.2	38.4 ± 3.0*#	39.9 ± 2.4
Σ n–6/Σ n–3		24.1 ± 3.9	18.5 ± 0.7*	18.9 ± 0.9*
Σ PUFA		43.1 ± 2.4	40.5 ± 3.2	42.1 ± 2.5
Σ SFA/Σ PUFA		0.53 ± 0.07	0.63 ± 0.08*	0.58 ± 0.06

Data are presented as means ± SE of the % of total fatty acids (FAs); $n = 6$ for each group. Ovx, ovariectomized; Ovx+E_2, ovariectomized with 17β-estradiol replacement; MUFA, monounsaturated fatty acids; PUFA, polyunsaturated fatty acids; RAT, retroperitoneal adipose depot; SFA, saturated fatty acids; Sham, sham operated. *$P < 0.05$ vs. Sham; #$P < 0.05$ Ovx vs. Ovx+E_2.

Ovariectomy increased body weight gain and adiposity due to increased feed efficiency, as food intake was not increased. Insulin and leptin levels, leptin-to-adiponectin ratio, and HOMA indexes also increased after ovariectomy, and these alterations were attenuated by the estradiol replacement therapy, as we have previously shown (5). The estrogen replacement dose was chosen as to be compatible with the human dosage of the average transdermal replacement therapy for postmenopausal women (22, 48).

The pathway analyses indicated that ovariectomy had a large impact on the metabolism of lipids, affecting the fatty acid metabolism/mitochondrial fatty-acid β-oxidation pathway and the fatty acyl-CoA biosynthesis pathway. Figure 5 depicts the main effects of ovariectomy in these pathways, which are addressed below.

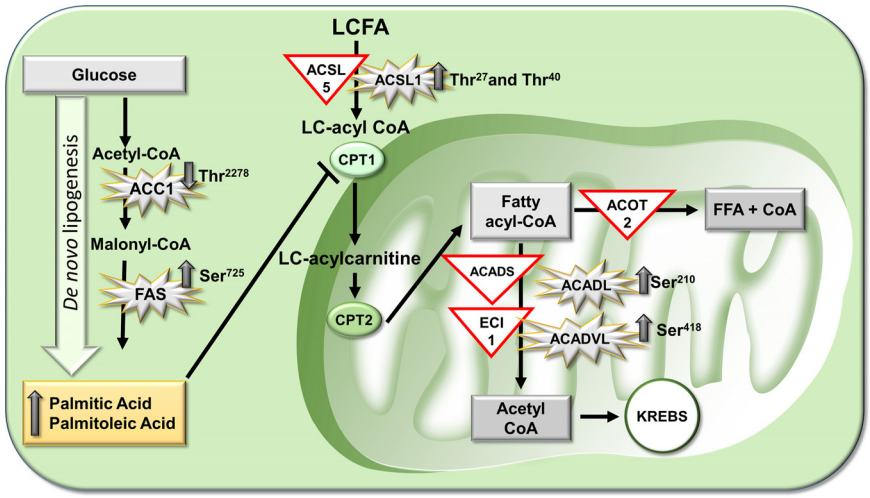

Fig. 5. Summary of the alterations in lipid metabolism induced by ovariectomy, as indicated by proteome/phosphoproteome analysis. Red triangles indicate reduced protein expression; Arrows followed by amino acid symbol indicate reduced (↓) or increased (↑) phosphorylation of the residue in the protein shown. ACADL, long-chain specific acyl-CoA dehydrogenase; ACADS, short-chain specific acyl-CoA dehydrogenase; ACADVL, very long-chain specific acyl-CoA dehydrogenase; ACC1, acetyl-CoA carboxylase-1; ACOT2, acyl-coenzyme A thioesterase type 2; ACSL1, long-chain fatty acid-CoA ligase 1; ACSL5, long-chain fatty acid-CoA ligase 5; ECI1, enoyl-CoA delta isomerase-1; FAS, fatty acid synthase; FFA, free fatty acids.

The activation of free fatty acids by their association with coenzyme A, yielding fatty-acyl CoA, is promoted by the ligase enzymes and represents a crucial step both for β-oxidation and synthesis of triacylglycerols and other lipids. In comparison to the Sham group, we observed downregulation of the protein ACSL5, a feature that has been associated with low β-oxidation rates (27), and increased phosphorylation of the protein (ACSL1). The present result on ACSL5 agrees with a previous report of its reduced gene expression in diabetic mice (32). The phosphorylation sites of the ACSL1 found in the present study (Thr^{27} and Thr^{40}) have not been reported previously, whereas a threonine phosphorylation site (Thr^{85}) was described in liver mitochondria of normal rats under physiological conditions (13).

The acyl-CoA dehydrogenases, responsible for fatty acyl-CoA desaturation in the β-oxidation pathway (19), also showed an effect of ovariectomy. The protein ACADS showed downregulation in comparison to the Sham group. This is in accordance with a report in the white adipose tissue from obese subjects (39). The ACADL and ACADVL proteins presented increased phosphorylation (Ser^{210} and Ser^{418}, respectively) compared with the Sham group. Although ACADVL has no phosphorylation sites previously reported, there is a previous description of decreased serine phosphorylation of ACADL (Ser^{28}/Ser^{30}) after ischemia in ovarian tumor grafts (41) and a demonstration that its decreased phosphorylation (Ser^{586}) in fibrotic lung cells was associated with higher lipid peroxidation in comparison to normal lung cells (24).

Two other enzymes of the mitochondrial fatty acid β-oxidation pathway, ACOT2 and ECI1, showed downregulation in response to ovariectomy. Located in the mitochondrial matrix, ACOT2 targets mainly long-chain fatty acyl-CoAs and catalyzes their hydrolysis to the free fatty acids and CoA. This mechanism has been proposed to enhance hepatic long-chain fatty acid oxidation by preventing accumulation of fatty acyl-CoA during high rates of hepatic β-oxidation (43, 61). ECI1 is involved in the process of oxidation of unsaturated fatty acids and has been reported to be downregulated in white adipose tissue from female Zucker diabetic fatty rats (34).

Ovariectomy also affected proteins involved in fatty acid synthesis. The protein ACC1 showed decreased phosphorylation at Thr^{2278}, attenuated by estradiol replacement. ACC1 converts acetyl-CoA into malonyl-CoA during de novo lipogenesis. Although the phosphorylation site found in the present study has not been previously described, the phosphorylation of at least other five sites was demonstrated to inhibit the protein activity, resulting in lower malonyl-CoA levels (18, 25). In addition, the protein FAS showed increased phosphorylation at Ser^{725} in comparison to the Sham group. FAS is a key enzyme in the lipogenesis process, catalyzing the conversion of malonyl-CoA to palmitic acid (59). FAS phosphorylation at Ser^{725} was increased in the liver of mice after refeeding, a situation favoring lipogenesis (65). Ovariectomy has been shown to increase FAS protein expression in the retroperitoneal adipose tissue of rats (31). The present observation that the lipid metabolism alterations induced by ovariectomy were attenuated by estradiol replacement agrees with a report of decreased lipogenesis by estradiol through inhibition of ACC1 and FAS (37).

Ovariectomy also modulated proteins involved in the adipogenesis process. The protein RETSAT showed increased expression and decreased phosphorylation in comparison to the Sham group. This protein favors adipocyte differentiation under normal metabolic conditions and was shown to be induced during adipogenesis, being positively regulated by the transcription factor peroxisome proliferator-activated receptor γ. Furthermore, the downregulation of the protein has been shown to inhibit adipogenesis (44, 57). Because the present Ovx animals showed increased body fat and mild increases in adipose tissue cytokine levels, it can be suggested that the upregulated RETSAT indicates a state of active fat accumulation. Moreover, further studies are necessary to elucidate the consequences of reduced phosphorylation of the sites found in the present study (Ser^{404}/Tyr^{409}).

The protein LPL showed increased expression and phosphorylation in the Ovx groups compared with the Sham group, indicating a high capacity of the retroperitoneal adipose tissue for uptake of lipoprotein-derived free fatty acids. This enzyme has also been implicated in adipocyte differentiation, and it has shown increased expression in adipose-derived mesenchymal stem cells from ovariectomized mice (17). Moreover, estrogens have been shown to decrease LPL expression in the subcutaneous fat of premenopausal women (52). Of note, we were not able to find previous records of the phosphorylation site found in the present study (Tyr^{191}).

Since ovariectomized animals were obese and showed alterations in many proteins involved in lipid metabolism, we hypothesized that fatty acid composition of RAT could be affected. Data about the effects of ovariectomy-induced obesity on fatty acid profile are scarce, although the proinflammatory state of common obesity has been associated to SFA in the adipose tissue (10). Our results showed increased palmitic acid and total SFA contents of RAT. Estrogen replacement was able to attenuate these effects. In postmenopausal obese women, visceral adipose tissue inflammation has been related to accumulation of SFA, especially palmitic acid (66). Although palmitic acid has been shown to impact fatty acid metabolism by upregulating the expression of ACSLs (47, 53), high levels have been found to lower fatty acid oxidation due to inhibition of carnitine-palmitoyltransferase 1A (33).

Ovariectomy also increased the percentage of the monounsaturated palmitoleic fatty acid. Endogenous nondietary palmitoleic acid originates mainly from de novo lipogenesis in white adipose tissue and has been recently considered a lipokine, since it is released from the tissue and acts on distant cells. However, its metabolic effects have not been elucidated, as both deleterious and beneficial effects on adiposity, insulin sensitivity, and lipid profile have been described (16). In the present study, its higher levels after ovariectomy are consistent with the proteomic results indicating a high lipogenesis rate, attenuated by estradiol replacement.

Regarding polyunsaturated fatty acids, our results showed a decrease in linoleic acid (n–6) and an increase in alpha-linolenic acid (n–3). Linoleic acid is a precursor of proinflammatory lipid mediators such as prostaglandins and leukotrienes (54). Although we did not measure these factors, it is fair to speculate that the decrease in linoleic acid in the ovariectomized animals was a consequence of its recruitment for the production of proinflammatory factors, since we had indications of an inflamed status induced by ovariectomy, as discussed above. Given the fact that the sum of PUFAs did not

differ among the groups, the increase in n–3 was a direct consequence of the n–6 decrease.

These present findings indicate that ovariectomy favored a disruption of fat metabolism, which may have been relevant in the development of obesity. However, on the basis of our observations it is not possible to rule out that, rather than a cause, the observed changes in lipid metabolism were a consequence of obesity.

The pathway analysis also showed that several proteins that take part in the innate immune system, which orchestrates inflammation (15), were modulated by ovariectomy. CD36 produced in macrophages is considered a proinflammatory marker. In the present study, this protein was upregulated by ovariectomy, in comparison to the Sham group, in agreement with findings in the visceral adipose tissue of postmenopausal women, obese individuals of both sexes, and the perivascular adipose tissue of diabetic rats (4, 30). CD36 is also involved in fatty acid translocation, thus influencing fat storage. Increased mRNA levels of CD36 in liver and visceral adipose tissue of ovariectomized mice have been associated with hepatic steatosis and increased visceral fat mass (50). Additionally, $CD36^{-/-}$ mice have shown enhanced fatty acid oxidation measured in muscle cell lines (55). These data agree with the present suggestion of impaired fatty acid oxidation in the visceral adipose tissue after ovariectomy.

Although they are not shown in the pathway analysis, it is relevant to note two other proteins altered by ovariectomy that have important inflammatory roles. The protein CAP1 showed increased expression and phosphorylation in comparison to the Sham group. In monocytes, this protein was described to function as a receptor for adipocyte-derived resistin, which in turn regulates inflammation signaling, leading to the release of proinflammatory cytokines. Its expression was found to be increased in cells extracted from white adipose tissue of obese humans (9). The phosphorylation at Thr^{306}/Ser^{307} identified in the present study was found to be increased in response to lipopolysaccharide-induced inflammation in macrophages (29), which corroborates the idea of an overall inflammatory status of our experimental model. Moreover, the protein RT1-AW2 also showed increased expression and phosphorylation in comparison to the Sham group. This protein is involved in immune response and was shown to be upregulated in the secretome of hepatocytes of rats treated with hepatocarcinogenic substances, a condition also associated with a proinflammatory environment (64). The phosphorylation site described in the present study (Ser^{295}) has not been described yet, but the Ser^{354} phosphorylation was found to be increased in liver mitochondria from obese mice (26). Estrogen replacement attenuated the ovariectomy-induced changes regarding the proteins CD36, CAP1, and RT1-AW2. These results are compatible with the increase in leptin levels as well as a decrease in leptin-to-adiponectin ratio and suggest an overall effect of estrogen replacement in reducing the inflammation status. This is compatible with reports that estradiol may regulate cell recruitment to inflammatory sites and decrease the production of proinflammatory cytokines, balancing the acute innate immune response (60).

Regarding the glucose metabolism impairment mentioned above, two proteins that play a role in insulin resistance were shown to be modulated by ovariectomy. One of them is EEF1D, which is involved in the protein elongation steps during the synthesis of a variety of proteins, acting in the regulation of translation and transcription (56). Insulin stimulates the activity of this enzyme, mainly through phosphorylation processes in adipose tissue, as observed after in vitro experiments using adipose-derived 3T3-L1 cells (8). The fact that this protein showed downregulated expression in the Ovx group compared with the Sham group is compatible with our suggestion of insulin resistance after ovariectomy. The other protein is ITB1, which showed decreased expression and increased phosphorylation induced by ovariectomy compared with the Sham group. The protein is localized in the cell membrane and participates in the signaling between extracellular matrix and the intracellular environment, and dysfunctional integrins have been related to insulin resistance (35). In visceral fat pads isolated from chow-fed rats, ITB1 potentiated the ability of insulin to enhance tyrosine phosphorylation of insulin receptor substrate 1 (21). Increased phosphorylation at Ser^{263} described in the present study has been previously found in breast cancer, but the consequences of this cancer-induced alteration for ITB1 function have not yet been explored (42). Since this modification appeared in the present study in an obese pathological condition, it may be not inferred whether it yielded a deleterious effect or, alternatively, whether it represented a counterregulatory mechanism to insulin resistance.

In conclusion, the present results indicate that ovariectomy favored lipogenesis whereas it impaired fatty acid oxidation and induced a proinflammatory state in the RAT. These effects are consistent with the findings of high adiposity, hyperleptinemia, and impaired insulin sensitivity. The observed alterations were partially attenuated by estradiol replacement. The data point to a role of disrupted lipid metabolism in adipose tissue in the genesis of obesity after menopause.

ACKNOWLEDGMENTS

The authors thank Mauro Cardoso Pereira for animal care, Nelson Inácio Pinto for assistance throughout the treatments, and Debora Estadella for contributions regarding creation of Fig. 4.

GRANTS

This study was financed by the Brazilian Agencies Coordenação de Aperfeiçoamento de Pessoal de Nível Superior (CAPES, Finance Code 001), Conselho Nacional de Desenvolvimento Científico e Tecnológico (CNPq, Grants 453924/2014-0 and 309505/2017-8), and Fundação de Amparo à Pesquisa do Estado de São Paulo (FAPESP, Grant No. 2012/03172-4, 2014/10068-4 and 2019/00098-7).

DISCLOSURES

No conflicts of interest, financial or otherwise, are declared by the authors.

AUTHOR CONTRIBUTIONS

V.T.B. and E.B.R. conceived and designed research; V.T.B., A.P.P., and C.B.-T. performed experiments; V.T.B., A.P.P., C.B.-T., E.G.L., A.A.B., and D.M.-dS. analyzed data; V.T.B., A.P.P., E.G.L., C.M.N., L.M.O., A.A.B., D.M.-dS., and E.B.R. interpreted results of experiments; V.T.B. prepared figures; V.T.B. drafted manuscript; V.T.B., A.P.P., and E.B.R. edited and revised manuscript; V.T.B., A.P.P., C.B.-T., E.G.L., C.M.N., L.M.O., A.A.B., D.M.-dS., and E.B.R. approved final version of manuscript.

REFERENCES

1. **Amengual-Cladera E, Lladó I, Gianotti M, Proenza AM.** Retroperitoneal white adipose tissue mitochondrial function and adiponectin expression in response to ovariectomy and 17β-estradiol replacement. *Steroids* 77: 659–665, 2012. doi:10.1016/j.steroids.2012.02.012.

2. **Amengual-Cladera E, Capllonch-Amer G, Lladó I, Gianotti M, Proenza AM.** Proteomic study of periovarian adipose tissue in 17β-estradiol-treated and untreated ovariectomized rats. *Biochem Cell Biol* 94: 167–175, 2016. doi:10.1139/bcb-2015-0077.
3. **Andersson T, Söderström I, Simonyté K, Olsson T.** Estrogen reduces 11beta-hydroxysteroid dehydrogenase type 1 in liver and visceral, but not subcutaneous, adipose tissue in rats. *Obesity (Silver Spring)* 18: 470–475, 2010. doi:10.1038/oby.2009.294.
4. **Azul L, Leandro A, Boroumand P, Klip A, Seiça R, Sena CM.** Increased inflammation, oxidative stress and a reduction in antioxidant defense enzymes in perivascular adipose tissue contribute to vascular dysfunction in type 2 diabetes. *Free Radic Biol Med* 146: 264–274, 2020. doi:10.1016/j.freeradbiomed.2019.11.002.
5. **Boldarine VT, Pedroso AP, Neto NI, Dornellas AP, Nascimento CM, Oyama LM, Ribeiro EB.** High-fat diet intake induces depressive-like behavior in ovariectomized rats. *Sci Rep* 9: 10551, 2019. doi:10.1038/s41598-019-47152-1.
6. **Bueno AA, Oyama LM, de Macedo Motoyama CS, da Silva Biz CR, Silveira VL, Ribeiro EB, Oller do Nascimento CM.** Long chain saturated fatty acids increase haptoglobin gene expression in C57BL/6J mice adipose tissue and 3T3-L1 cells. *Eur J Nutr* 49: 235–241, 2010. doi:10.1007/s00394-009-0069-z.
7. **Bueno AA, Ghebremeskel K, Bakheit KH, Elbashir MI, Adam I.** Dimethyl acetals, an indirect marker of the endogenous antioxidant plasmalogen level, are reduced in blood lipids of Sudanese pre-eclamptic subjects whose background diet is high in carbohydrate. *J Obstet Gynaecol* 32: 241–246, 2012. doi:10.3109/01443615.2011.641622.
8. **Chang YW, Traugh JA.** Insulin stimulation of phosphorylation of elongation factor 1 (eEF-1) enhances elongation activity. *Eur J Biochem* 251: 201–207, 1998. doi:10.1046/j.1432-1327.1998.2510201.x.
9. **Choi MS, Kim YJ, Kwon EY, Ryoo JY, Kim SR, Jung UJ.** High-fat diet decreases energy expenditure and expression of genes controlling lipid metabolism, mitochondrial function and skeletal system development in the adipose tissue, along with increased expression of extracellular matrix remodelling- and inflammation-related genes. *Br J Nutr* 113: 867–877, 2015. doi:10.1017/S0007114515000100.
10. **Cusi K.** The role of adipose tissue and lipotoxicity in the pathogenesis of type 2 diabetes. *Curr Diab Rep* 10: 306–315, 2010. doi:10.1007/s11892-010-0122-6.
11. **Dalal PK, Agarwal M.** Postmenopausal syndrome. *Indian J Psychiatry* 57, *Suppl* 2: 222–232, 2015. doi:10.4103/0019-5545.161483.
12. **de Souza CF, Stopa LR, Santos GF, Takasumi LC, Martins AB, Garnica-Siqueira MC, Ferreira RN, de Andrade FG, Leite CM, Zaia DA, Zaia CT, Uchoa ET.** Estradiol protects against ovariectomy-induced susceptibility to the anabolic effects of glucocorticoids in rats. *Life Sci* 218: 185–196, 2019. doi:10.1016/j.lfs.2018.12.037.
13. **Distler AM, Kerner J, Hoppel CL.** Post-translational modifications of rat liver mitochondrial outer membrane proteins identified by mass spectrometry. *Biochim Biophys Acta* 1774: 628–636, 2007. doi:10.1016/j.bbapap.2007.03.012.
14. **Dornellas APS, Boldarine VT, Pedroso AP, Carvalho LO, de Andrade IS, Vulcani-Freitas TM, Dos Santos CC, do Nascimento CM, Oyama LM, Ribeiro EB.** High-fat feeding improves anxiety-type behavior induced by ovariectomy in rats. *Front Neurosci* 12: 557, 2018. [Erratum in *Front Neurosci* 12: 738, 2018.] doi:10.3389/fnins.2018.00557.
15. **Eaton SA, Sethi JK.** Immunometabolic links between estrogen, adipose tissue and female reproductive metabolism. *Biology (Basel)* 8: 8, 2019. doi:10.3390/biology8010008.
16. **Frigolet ME, Gutiérrez-Aguilar R.** The role of the novel lipokine palmitoleic acid in health and disease. *Adv Nutr* 8: 173S–181S, 2017. doi:10.3945/an.115.011130.
17. **Fu Y, Li R, Zhong J, Fu N, Wei X, Cun X, Deng S, Li G, Xie J, Cai X, Lin Y.** Adipogenic differentiation potential of adipose-derived mesenchymal stem cells from ovariectomized mice. *Cell Prolif* 47: 604–614, 2014. doi:10.1111/cpr.12131.
18. **Galic S, Loh K, Murray-Segal L, Steinberg GR, Andrews ZB, Kemp BE.** AMPK signaling to acetyl-CoA carboxylase is required for fasting- and cold-induced appetite but not thermogenesis. *eLife* 7: e32656, 2018. doi:10.7554/eLife.32656.
19. **Ghisla S, Thorpe C.** Acyl-CoA dehydrogenases. A mechanistic overview. *Eur J Biochem* 271: 494–508, 2004. doi:10.1046/j.1432-1033.2003.03946.x.
20. **Goettems-Fiorin PB, Costa-Beber LC, Dos Santos JB, Friske PT, Sulzbacher LM, Frizzo MN, Ludwig MS, Rhoden CR, Heck TG.** Ovariectomy predisposes female rats to fine particulate matter exposure's effects by altering metabolic, oxidative, pro-inflammatory, and heat-shock protein levels. *Environ Sci Pollut Res Int* 26: 20581–20594, 2019. doi:10.1007/s11356-019-05383-9.
21. **Guilherme A, Torres K, Czech MP.** Cross-talk between insulin receptor and integrin alpha5 beta1 signaling pathways. *J Biol Chem* 273: 22899–22903, 1998. doi:10.1074/jbc.273.36.22899.
22. **Hill DA, Crider M, Hill SR.** Hormone therapy and other treatments for symptoms of menopause. *Am Fam Physician* 94: 884–889, 2016.
23. **Horber FF, Gruber B, Thomi F, Jensen EX, Jaeger P.** Effect of sex and age on bone mass, body composition and fuel metabolism in humans. *Nutrition* 13: 524–534, 1997. doi:10.1016/S0899-9007(97)00031-2.
24. **Kabuyama Y, Suzuki T, Nakazawa N, Yamaki J, Homma MK, Homma Y.** Dysregulation of very long chain acyl-CoA dehydrogenase coupled with lipid peroxidation. *Am J Physiol Cell Physiol* 298: C107–C113, 2010. doi:10.1152/ajpcell.00231.2009.
25. **Kim KH, López-Casillas F, Bai DH, Luo X, Pape ME.** Role of reversible phosphorylation of acetyl-CoA carboxylase in long-chain fatty acid synthesis. *FASEB J* 3: 2250–2256, 1989. doi:10.1096/fasebj.3.11.2570725.
26. **Klepeisz P, Sagmeister S, Haudek-Prinz V, Pichlbauer M, Grasl-Kraupp B, Gerner C.** Phenobarbital induces alterations in the proteome of hepatocytes and mesenchymal cells of rat livers. *PLoS One* 8: e76137, 2013. doi:10.1371/journal.pone.0076137.
27. **Knights KM.** Role of hepatic fatty acid:coenzyme A ligases in the metabolism of xenobiotic carboxylic acids. *Clin Exp Pharmacol Physiol* 25: 776–782, 1998. doi:10.1111/j.1440-1681.1998.tb02152.x.
28. **Kozakowski J, Gietka-Czernel M, Leszczyńska D, Majos A.** Obesity in menopause—our negligence or an unfortunate inevitability? *Przegl Menopauz* 16: 61–65, 2017. doi:10.5114/pm.2017.68594.
29. **Lee S, Lee HC, Kwon YW, Lee SE, Cho Y, Kim J, Lee S, Kim JY, Lee J, Yang HM, Mook-Jung I, Nam KY, Chung J, Lazar MA, Kim HS.** Adenylyl cyclase-associated protein 1 is a receptor for human resistin and mediates inflammatory actions of human monocytes. *Cell Metab* 19: 484–497, 2014. doi:10.1016/j.cmet.2014.01.013.
30. **Lesna IK, Cejkova S, Kralova A, Fronek J, Petras M, Sekerkova A, Thieme F, Janousek L, Poledne R.** Human adipose tissue accumulation is associated with pro-inflammatory changes in subcutaneous rather than visceral adipose tissue. *Nutr Diabetes* 7: e264, 2017. doi:10.1038/nutd.2017.15.
31. **Leu SY, Chen YC, Tsai YC, Hung YW, Hsu CH, Lee YM, Cheng PY.** Raspberry ketone reduced lipid accumulation in 3T3–L1 cells and ovariectomy-induced obesity in Wistar rats by regulating autophagy mechanisms. *J Agric Food Chem* 65: 10907–10914, 2017. doi:10.1021/acs.jafc.7b03831.
32. **Lewin TM, Kim JH, Granger DA, Vance JE, Coleman RA.** Acyl-CoA synthetase isoforms 1, 4, and 5 are present in different subcellular membranes in rat liver and can be inhibited independently. *J Biol Chem* 276: 24674–24679, 2001. doi:10.1074/jbc.M102036200.
33. **Li P, Liu Y, Zhang Y, Long M, Guo Y, Wang Z, Li X, Zhang C, Li X, He J, Liu G.** Effect of non-esterified fatty acids on fatty acid metabolism-related genes in calf hepatocytes cultured in vitro. *Cell Physiol Biochem* 32: 1509–1516, 2013. doi:10.1159/000356588.
34. **Liang Y, She P, Wang X, Demarest K.** The messenger RNA profiles in liver, hypothalamus, white adipose tissue, and skeletal muscle of female Zucker diabetic fatty rats after topiramate treatment. *Metabolism* 55: 1411–1419, 2006. doi:10.1016/j.metabol.2006.06.013.
35. **Lin D, Chun TH, Kang L.** Adipose extracellular matrix remodelling in obesity and insulin resistance. *Biochem Pharmacol* 119: 8–16, 2016. doi:10.1016/j.bcp.2016.05.005.
36. **Lin Y, Huo L, Liu Z, Li J, Liu Y, He Q, Wang X, Liang S.** Sodium laurate, a novel protease- and mass spectrometry-compatible detergent for mass spectrometry-based membrane proteomics. *PLoS One* 8: e59779, 2013. doi:10.1371/journal.pone.0059779.
37. **López M, Tena-Sempere M.** Estradiol effects on hypothalamic AMPK and BAT thermogenesis: a gateway for obesity treatment? *Pharmacol Ther* 178: 109–122, 2017. doi:10.1016/j.pharmthera.2017.03.014.
38. **Luong Q, Huang J, Lee KY.** Deciphering white adipose tissue heterogeneity. *Biology (Basel)* 8: 23, 2019. doi:10.3390/biology8020023.
39. **Marrades MP, González-Muniesa P, Arteta D, Martínez JA, Moreno-Aliaga MJ.** Orchestrated downregulation of genes involved in oxidative metabolic pathways in obese vs. lean high-fat young male consumers. *J Physiol Biochem* 67: 15–26, 2011. doi:10.1007/s13105-010-0044-4.

40. **Mathis D, Shoelson SE.** Immunometabolism: an emerging frontier. *Nat Rev Immunol* 11: 81–83, 2011. doi:10.1038/nri2922.
41. **Mertins P, Yang F, Liu T, Mani DR, Petyuk VA, Gillette MA, Clauser KR, Qiao JW, Gritsenko MA, Moore RJ, Levine DA, Townsend R, Erdmann-Gilmore P, Snider JE, Davies SR, Ruggles KV, Fenyo D, Kitchens RT, Li S, Olvera N, Dao F, Rodriguez H, Chan DW, Liebler D, White F, Rodland KD, Mills GB, Smith RD, Paulovich AG, Ellis M, Carr SA.** Ischemia in tumors induces early and sustained phosphorylation changes in stress kinase pathways but does not affect global protein levels. *Mol Cell Proteomics* 13: 1690–1704, 2014. doi:10.1074/mcp.M113.036392.
42. **Mertins P, Mani DR, Ruggles KV, Gillette MA, Clauser KR, Wang P, Wang X, Qiao JW, Cao S, Petralia F, Kawaler E, Mundt F, Krug K, Tu Z, Lei JT, Gatza ML, Wilkerson M, Perou CM, Yellapantula V, Huang KL, Lin C, McLellan MD, Yan P, Davies SR, Townsend RR, Skates SJ, Wang J, Zhang B, Kinsinger CR, Mesri M, Rodriguez H, Ding L, Paulovich AG, Fenyö D, Ellis MJ, Carr SA; NCI CPTAC.** Proteogenomics connects somatic mutations to signalling in breast cancer. *Nature* 534: 55–62, 2016. doi:10.1038/nature18003.
43. **Moffat C, Bhatia L, Nguyen T, Lynch P, Wang M, Wang D, Ilkayeva OR, Han X, Hirschey MD, Claypool SM, Seifert EL.** Acyl-CoA thioesterase-2 facilitates mitochondrial fatty acid oxidation in the liver. *J Lipid Res* 55: 2458–2470, 2014. doi:10.1194/jlr.M046961.
44. **Moise AR, Kuksa V, Imanishi Y, Palczewski K.** Identification of all-*trans*-retinol:all-*trans*-13,14-dihydroretinol saturase. *J Biol Chem* 279: 50230–50242, 2004. doi:10.1074/jbc.M409130200.
45. **Monteiro R, Teixeira D, Calhau C.** Estrogen signaling in metabolic inflammation. *Mediators Inflamm* 2014: 615917, 2014. doi:10.1155/2014/615917.
46. **Moreno MF, De Laquila R, Okuda MH, Lira FS, de Souza GI, de Souza CT, Telles MM, Ribeiro EB, do Nascimento CM, Oyama LM.** Metabolic profile response to administration of epigallocatechin-3-gallate in high-fat-fed mice. *Diabetol Metab Syndr* 6: 84, 2014. doi:10.1186/1758-5996-6-84.
47. **Nakakuki M, Kawano H, Notsu T, Imada K.** Eicosapentaenoic acid suppresses palmitate-induced cytokine production by modulating long-chain acyl-CoA synthetase 1 expression in human THP-1 macrophages. *Atherosclerosis* 227: 289–296, 2013. doi:10.1016/j.atherosclerosis.2012.12.036.
48. **Nair AB, Jacob S.** A simple practice guide for dose conversion between animals and human. *J Basic Clin Pharm* 7: 27–31, 2016. doi:10.4103/0976-0105.177703.
49. **Neto NI, Rodrigues ME, Hachul AC, Moreno MF, Boldarine VT, Ribeiro EB, Oyama LM, Oller do Nascimento CM.** A hyperlipidic diet combined with short-term ovariectomy increases adiposity and hyperleptinemia and decreases cytokine content in mesenteric adipose tissue. *Mediators Inflamm* 2015: 923248, 2015. doi:10.1155/2015/923248.
50. **Nishio E, Hayashi T, Nakatani M, Aida N, Suda R, Fujii T, Wakatsuki T, Honda S, Harada N, Shimono Y.** Lack of association of ovariectomy-induced obesity with overeating and the reduction of physical activities. *Biochem Biophys Rep* 20: 100671, 2019. doi:10.1016/j.bbrep.2019.100671.
51. **Pasing Y, Colnoe S, Hansen T.** Proteomics of hydrophobic samples: fast, robust and low-cost workflows for clinical approaches. *Proteomics* 17: 1500462, 2017. doi:10.1002/pmic.201500462.
52. **Price TM, O'Brien SN, Welter BH, George R, Anandjiwala J, Kilgore M.** Estrogen regulation of adipose tissue lipoprotein lipase—possible mechanism of body fat distribution. *Am J Obstet Gynecol* 178: 101–107, 1998. doi:10.1016/S0002-9378(98)70634-9.
53. **Rajkumar A, Liaghati A, Chan J, Lamothe G, Dent R, Doucet É, Rabasa-Lhoret R, Prud'homme D, Harper ME, Tesson F.** ACSL5 genotype influence on fatty acid metabolism: a cellular, tissue, and whole-body study. *Metabolism* 83: 271–279, 2018. doi:10.1016/j.metabol.2018.03.019.
54. **Robichaud PP, Surette ME.** Polyunsaturated fatty acid-phospholipid remodeling and inflammation. *Curr Opin Endocrinol Diabetes Obes* 22: 112–118, 2015. doi:10.1097/MED.0000000000000138.
55. **Samovski D, Sun J, Pietka T, Gross RW, Eckel RH, Su X, Stahl PD, Abumrad NA.** Regulation of AMPK activation by CD36 links fatty acid uptake to β-oxidation. *Diabetes* 64: 353–359, 2015. doi:10.2337/db14-0582.
56. **Sanders J, Raggiaschi R, Morales J, Möller W.** The human leucine zipper-containing guanine-nucleotide exchange protein elongation factor-1 delta. *Biochim Biophys Acta* 1174: 87–90, 1993. doi:10.1016/0167-4781(93)90097-W.
57. **Schupp M, Lefterova MI, Janke J, Leitner K, Cristancho AG, Mullican SE, Qatanani M, Szwergold N, Steger DJ, Curtin JC, Kim RJ, Suh MJ, Albert MR, Engeli S, Gudas LJ, Lazar MA.** Retinol saturase promotes adipogenesis and is downregulated in obesity. *Proc Natl Acad Sci USA* 106: 1105–1110, 2009. [Erratum in *Proc Natl Acad Sci USA* 106: 4571, 2009.] doi:10.1073/pnas.0812065106.
58. **Silva JC, Denny R, Dorschel CA, Gorenstein M, Kass IJ, Li GZ, McKenna T, Nold MJ, Richardson K, Young P, Geromanos S.** Quantitative proteomic analysis by accurate mass retention time pairs. *Anal Chem* 77: 2187–2200, 2005. doi:10.1021/ac048455k.
59. **Solinas G, Borén J, Dulloo AG.** De novo lipogenesis in metabolic homeostasis: more friend than foe? *Mol Metab* 4: 367–377, 2015. doi:10.1016/j.molmet.2015.03.004.
60. **Stubelius A, Andersson A, Islander U, Carlsten H.** Ovarian hormones in innate inflammation. *Immunobiology* 222: 878–883, 2017. doi:10.1016/j.imbio.2017.05.007.
61. **Tillander V, Alexson SE, Cohen DE.** Deactivating fatty acids: acyl-CoA thioesterase-mediated control of lipid metabolism. *Trends Endocrinol Metab* 28: 473–484, 2017. doi:10.1016/j.tem.2017.03.001.
62. **Trujillo ME, Scherer PE.** Adipose tissue-derived factors: impact on health and disease. *Endocr Rev* 27: 762–778, 2006. doi:10.1210/er.2006-0033.
63. **Weijers RN.** Lipid composition of cell membranes and its relevance in type 2 diabetes mellitus. *Curr Diabetes Rev* 8: 390–400, 2012. doi:10.2174/157339912802083531.
64. **Weintz G, Olsen JV, Frühauf K, Niedzielska M, Amit I, Jantsch J, Mages J, Frech C, Dölken L, Mann M, Lang R.** The phosphoproteome of toll-like receptor-activated macrophages. *Mol Syst Biol* 6: 371, 2010. doi:10.1038/msb.2010.29.
65. **Wilson-Grady JT, Haas W, Gygi SP.** Quantitative comparison of the fasted and re-fed mouse liver phosphoproteomes using lower pH reductive dimethylation. *Methods* 61: 277–286, 2013. doi:10.1016/j.ymeth.2013.03.031.
66. **Yamatani H, Takahashi K, Yoshida T, Takata K, Kurachi H.** Association of estrogen with glucocorticoid levels in visceral fat in postmenopausal women. *Menopause* 20: 437–442, 2013.
67. **Yamatani H, Takahashi K, Yoshida T, Soga T, Kurachi H.** Differences in the fatty acid metabolism of visceral adipose tissue in postmenopausal women. *Menopause* 21: 170–176, 2014. doi:10.1097/GME.0b013e318296431a.